REVIEW ARTICLE
DOI: https://doi.org/10.18502/fem.v7i3.13825

Diagnostic accuracy of inverted grayscale mode in radiographs: a systematic review and meta–analysis

Mohammad Eftekhari[1], Mohammad Jalili[1], Amirhossein Karim[1], Amin Doosti–Irani[2], Hadi Mirfazaelian[1]*

1. Department of Emergency Medicine, Tehran University of Medical Sciences, Tehran, Iran.

2. Department of Epidemiology, School of Public Health and Modeling of Non–communicable Diseases Research Center, Hamadan University of Medical Sciences, Hamadan, Iran.

***Corresponding author:** Hadi Mirfazaelian; **Email:** H-mirfazaelian@sina.tums.ac.ir

Published online: 2023–03–11

Abstract: X–rays are routinely utilized for different diagnostic purposes but there is always the risk of an inaccurate diagnosis. This systematic review was designed to investigate whether inverse grayscale mode increased diagnostic accuracy. From inception to February 2022, MEDLINE, Embase, Scopus, Web of Science, and CENTRAL were searched for studies comparing grayscale inversion diagnostic accuracy to the conventional method. Quality assessment was performed using the Quality Assessment of Diagnostic Accuracy Studies version 2 (QUADAS–2) tool. Eighteen studies were included with an overall patient population of 1704. The number of studies investigating each lesion are as follows, lung masses: 13, pneumothoraces: 4, bony lesions: 3, interstitial lung diseases: 3, orthopedic studies: 2, bullous lung disease: 1, pleural effusion: 1, urinary calculus: 1, and large vascular occlusion: 1. Two studies had an overall moderate risk of bias and the remainders had low risk. The combined mode, featuring the conventional mode with the addition of the inverse grayscale, demonstrated better performance or insignificant difference in comparison with the conventional mode in all studies except one, which showed lower sensitivity in detecting pulmonary nodules. Also, meta–analysis of 250 patients in four pulmonary nodule studies showed better area under the ROC curve (AUC) of inverse mode (0.83, 95% CI: 0.75,0.90) in comparison with conventional mode (0.80, 95% CI: 0.72,0.88). Application of inverse mode when using radiography for detection of pulmonary nodules might improve diagnostic accuracy. Also, the inverse/combined mode showed better performance for lesions other than pulmonary nodule in some studies. However, there was insufficient evidence to draw a consistent conclusion.

Keywords: Accuracy; Image Processing; Radiograph

Cite this article as: Eftekhari M, Jalili M, Karim A, Doosti–Irani A, Mirfazaelian H. Diagnostic accuracy of inverted grayscale mode in radiographs: a systematic review and meta–analysis. Front Emerg Med. In Press.

1. Introduction

Worldwide, there is an estimated four percent error rate when interpreting X–ray images (1). To reduce misdiagnoses, different strategies have been utilized with variable success. Grayscale inversion has been hypothesized to improve human perception by analyzing dark objects against a white background, inverse mode, as opposed to the opposite, conventional mode (2,3). This concept was investigated in few studies during years by sophisticated devices such as hard–copy radiographs or secondary digitized images. Image processing has become as easy as just one click after emerging Picture Archiving Communication System (PACS) (4,5). This in turn has brought attention back to the question of how utilization of the inverse mode may affect the accuracy of practitioners in interpreting the images. Despite several studies, no firm conclusion has yet arrived.

This systematic review study assessed observer performance in X–ray interpretation between the inverse mode and conventional mode.

2. Methods

2.1. Criteria for including studies for this review

This systematic review included all English studies that compared the inverse mode against the conventional mode when evaluating observer performance, regardless of the study location or publication year.

We exclude studies that investigated only intra– and/or inter–observer reliabilities but not the accuracy, studies with results without clear definition of parameters, and also case report(s).

2.2. Search strategy

We employed a librarian with expertise in systematic review to develop search terms that included an extensive controlled vocabulary and keyword searches. We incorporated the following texts in the search strategy: 'grey–scale', 'greyscale', 'grayscale', 'gray–scale', 'inver*', 'revers*', 'conver*', 'sensitivity', 'specificity', 'diagnos*' and 'accuracy of detection'. The following databases were included in the elec-

Copyright © 2023 Tehran University of Medical Sciences
This work is licensed under a Creative Commons Attribution-NonCommercial 4.0 International license (https://creativecommons.org /licenses/by-nc/4.0/). Noncommercial uses of the work are permitted, provided the original work is properly cited.

tronic search from inception to February 2022: MEDLINE, Embase, Scopus, Web of Science, and CENTRAL. We also excluded nonmedical radiograph applications including dentistry. In addition, the reference lists and citations of the included studies were reviewed for additional sources. The search strategy is noted on appendix 1.

2.3. Data extraction and quality assessment

Two authors (ME and AK) independently screened titles and abstracts of potentially relevant articles after the exclusion of duplicates. The conflicts were resolved by a third investigator (HM). Next, full texts were scrutinized for inclusion in the final analysis. The following data were extracted: the first author of the paper, year of publication, country, sample size, inclusion and exclusion criteria, diagnostic gold standard, and performance indicators including sensitivity, specificity, positive and negative predictive values, positive and negative likelihood ratios, and accuracy.

2.4. Quality assessment

Included studies were independently examined for study quality using the Quality Assessment of Diagnostic Accuracy Studies version 2 (QUADAS–2) tool, which provides an objective and transparent rating of bias and applicability for diagnostic accuracy studies. Four domains are used to assess for bias: patient selection, index text, reference standard, as well as flow and timing.
Risk of bias was classified as low, high, or unclear for each of the four domains (6). Data was then extracted to construct contingency tables.

2.5. Data synthesis

We pooled the sensitivity, specificity, and estimated area under the curve (AUC) using meta–analysis. The random effects model was used for reporting the results.
The statistical heterogeneity among the results of included studies was assessed by using the chi–squared test (Q–statistic) and quantified by I2 (a parameter that describes the percentage of total variation across studies attributable to heterogeneity, rather than chance) and Tau squared (7). Results were reported at a 95% confidence interval (CI). Stata version 11 (Stata Corp, College Station, Texas, USA) was used for data analysis.
The recommendation in this study is rated according to grading of recommendations, assessment, development and evaluations (GRADE) guideline (8).

3. Results

3.1. Description of included studies

The search yielded 1068 records, and after excluding duplicates, 549 records remained. Of these, 518 were excluded because the studies were either not written in English (9,10), related to the field of dentistry (11–17), or consisted of an irrelevant title and/or abstract (509). Thirty–one studies were scrutinized in full text. Five studies were excluded due to unrelated text (18–22), three due to evaluation of the intra/inter–observer correlation instead of accuracy (23–25), one study with no clear definition of inclusion criteria, gold standard, and measured parameters (26), and one case report study (27). In the end, 21 studies remained with a total patient population of 2321 (Figure 1).
Nine studies were conducted in Europe, six in Asia, five in North America, and one in Australia. The number of studies investigating each lesion are as follows, lung masses: 13, pneumothoraces: 4, bony lesions: 3, interstitial lung diseases: 3, orthopedic studies: 2, bullous lung disease: 1, pleural effusion: 1, urinary calculus: 1, and emergent large vessel occlusion (ELVO): 1 (Table 1).
Six studies applied inverse mode in addition to conventional mode (4,5,28–30). Of note, six studies used simulated abnormalities as either all or part of their patient population (3, 30–34).

3.2. Risk of bias

The patient selection domain was rated as high risk in one study where control images were not included and the readers were aware that all images were abnormal (35). Additionally, some studies included more difficult images defined as those containing abnormalities not diagnosed by novice interpreters (36–38). The patient selection domain in these studies were classified as low risk. However, one study that excluded pulmonary nodules in the central part of the chest was rated as high risk. This was due to the fact that there was not a clear definition for "central part"(39). Also, another study merely evaluated linear lesions in interstitial lung diseases (ILD) s and excluded ground–glass areas of attenuation, alveolar opacities, and prominent perivascular haziness without explaining the reason. As a result, we rated the patient selection domain as unclear risk of bias. The index test domain was unclear for only a single study due to residents with unknown experiences interpreting the images (38). The flow risk domain of two studies was rated as unclear because they used different reference standards. Other domains of bias and applicability in the remaining studies were classified as low (Table 2).

3.3. Diagnostic accuracy of inverse mode

Among thirteen studies on pulmonary nodules, six failed to show any significant difference between the two modes, three studies demonstrated lower performance of the inverse mode in all parameters, three other studies demonstrated improved performance of the inverse mode in all parameters (29,32,34); Furthermore, Lungren et al. obtained lower sensitivity and higher specificity for the inverse mode (Table 3).
Regarding lung regions obscured by mediastinum and/or diaphragm, two studies showed inconsistent results. In Kehler et al., inverse mode had an insignificantly lower accuracy (31) while Lungren et al. study showed significant higher accuracy for inverse and combined modes (30).

Copyright © 2023 Tehran University of Medical Sciences
This work is licensed under a Creative Commons Attribution-NonCommercial 4.0 International license (https://creativecommons.org /licenses/by-nc/4.0/).
Noncommercial uses of the work are permitted, provided the original work is properly cited.

Table 1 Included studies characteristics

Study (Y/C)	Sample size (case/ control)	Type of disease	Inclusion criteria	Exclusion criteria	Control group	Index test reader(s)	Reference test(s)	Comment(s)
Oestmann et al. (1987/US)	92 (46/46)	Lung cancer	Among 500 localized lung cancers seen on radiographs and proved by means of percutaneous needle aspiration biopsy	–	Selected from radiographs that were initially reported as normal and that were corroborated as normal at follow–up radiographic and clinical studies performed at least 2 years later	CXR Radiologists: 2 were radiologists with>15y, and 1 with 6 y of experience	Lung biopsy	Subtle cases
MacMahon et al. (1987/US)	60 patients, 120 hemithoraces (25/95)	• Pulmonary nodule • PTX • Interstitial infiltrates • Bone lesions (recent Fx or tumor involvement)	–	–	–	CXR *Twelve radiologists (6 staff radiologists and 6 senior radiology residents)	Two experienced radiologists and chest CT scan$^{\beta}$ and follow– up	• All abnormalities were visually subtle • Some hemithoraces included more than one type of abnormality
Oestmann et al. (1988/US)	100 (50/50)	Simulated nodule (random nodule sizes)	–	–	–	CXR Five board certified radiologists	Five board certified radiologists	Also evaluates edge enhancement
Sheline et al. (1988/US)	40 (25/15)	Pulmonary nodule	Pathologically proved pulmonary malignancy patients; pulmonary tumor had been missed when the films were interpreted routinely	–	Healthy people who had follow–up for several years to establish the absence of a tumor	CXR Six radiology residents in–training	Three radiologists	–
Kheddache S et al. (1991/Sweden)	200 (100/100)	• Pulmonary nodule • PTX	Simulated small & large nodules and PTX in an anthropomorphic chest phantom	–	–	CXR • Step 1(5 observers): 3 radiologists, 1 medical physicist, 1 student of radiation physics • Step 2 (5 observers): 3 radiologists, 1 pulmonologist, 1 medical physicist	Radiologists	• Step 1a: without any other image processing than grey–scale reversal with fixed monitor settings • Step1b: without any other image processing than grey–scale reversal with fixed monitor settings • Step 2: with image processing including edge and contrast enhancement

Copyright © 2023 Tehran University of Medical Sciences
This work is licensed under a Creative Commons Attribution-NonCommercial 4.0 International license (https://creativecommons.org /licenses/by-nc/4.0/). Noncommercial uses of the work are permitted, provided the original work is properly cited.

Table 1 Included studies characteristics (continued)

Study (Y/C)	Sample size (case/ control)	Type of disease	Inclusion criteria	Exclusion criteria	Control group	Index test reader(s)	Reference test(s)	Comment(s)
Kehler et al. (1991/Sweden)	80 real images (40/40) 100 phantom images (69/31)	Chest neoplasm	Chest tumor	The images with obvious lesions that all observers detected them, were excluded.	–	CXR Five radiologists • For real images: 1 experienced chest radiologist, 2 general specialists just starting specialization in chest radiology, and 2 residents • For phantom images: 3 experienced chest radiologists, informed of the size and appearance of the 2 test objects in the mediastinum and left lung	Radiologists	All images were with edge enhancement
Schaefer et al. (1991/US)	65 (40/25)	ILD	The criteria used for the diagnosis of interstitial abnormality consisted of irregular, linear, or honeycomb areas of attenuation that were widely distributed in one or both lungs	Ground glass areas of attenuation, alveolar opacities, and prominent perivascular haziness, which can also be manifestations of interstitial lung abnormality and atelectasis and bronchiectasis	Six patients with asbestos–related pleural disease and five patients with mediastinal adenopathy who had no parenchymal abnormality; the remainder had entirely normal lungs	CXR Six board certified radiologists	Chest CT scan	Also evaluated edge enhancement
Buckley1 et al. (1991/US)	60 (35/25)	Bullous lung disease	The identification of discrete, localized areas of low attenuation surrounded by well–defined, paper–thin mar-gins consisting of inverted pleura or compressed lung parenchyma or both. In some cases the bullae were surrounded by diffuse emphysema, but in most cases, they were located within otherwise normal parenchyma	Other causes of localized hyperinflation (e.g., honeycomb lung, bronchiectasis, or oligemia) were specifically excluded	–	CXR Six board–certified radiologists	Chest CT scan	Also evaluates edge enhancement

Copyright © 2023 Tehran University of Medical Sciences
This work is licensed under a Creative Commons Attribution-NonCommercial 4.0 International license (https://creativecommons.org /licenses/by-nc/4.0/). Noncommercial uses of the work are permitted, provided the original work is properly cited.

Table 1 Included studies characteristics (continued)

Study (Y/C)	Sample size (case/control)	Type of disease	Inclusion criteria	Exclusion criteria	Control group	Index test reader(s)	Reference test(s)	Comment(s)
Choi et al. (2002/Korea)	80 (40/40)	Pulmonary nodule	Small, non–calcified solitary pulmonary nodule (approximately 1cm in maximum diameter)	Two board–certified radiologists with at least 8 y clinical experience, screened each image to ensure that the following specifications were met: acceptable diagnostic quality; acquired no more than two weeks before or after CT scan examinations; no evidence of other pulmonary parenchymal abnormalities	–	CXR Ten radiologists participated in this study; 6 were board–certified radiologists and 4 were senior residents	Chest CT scan	–
KANG et al. (2004/South Korea)	75 (60/15)	Urinary calculi	Single urinary calculus <5mm in the long diameter (15 in the kidney; 15 in the proximal ureter; 15 in the mid–ureter, 15 in the distal ureter)	–	–	Abdominal X–ray Four radiologists: the 1^{st} and 2^{nd} readers were board–certificated radiologists with 7 y of experience in interpreting soft–copy abdominal radiographs for urinary calculus detection and who were familiar with reversed display. The 3^{rd} reader was a second–year resident who had completed 2 m of training schedule in the genitourinary division of the radiology department, familiar with reversed display of soft–copy abdominal radiographs for detection of urinary calculi. The 4^{th} reader was another second–year resident who had not yet undergone training in genitourinary division	• Four positive cases: unenhanced helical CT scan, excretory urography, and ureteroscopic findings • Four control cases: unenhanced helical CT scan	All control cases were from ER
De Boo et al. (2011/The Netherlands)	128 (74/54)	Pulmonary nodule	CT scan–proven non–calcified nodular opacities with diameters between 5 and 30 mm	–	–	CXR Six readers: 3 radiology residents (1^{st} to 3^{rd} y of training) and 3 board–certified radiologists (all with>10 y of experience)	Chest CT scan	–

Copyright © 2023 Tehran University of Medical Sciences
This work is licensed under a Creative Commons Attribution-NonCommercial 4.0 International license (https://creativecommons.org /licenses/by-nc/4.0/). Noncommercial uses of the work are permitted, provided the original work is properly cited.

Table 1 Included studies characteristics (continued)

Study (Y/C)	Sample size (case/ control)	Type of disease	Inclusion criteria	Exclusion criteria	Control group	Index test reader(s)	Reference test(s)	Comment(s)
Lungren et al. (2011/US)	144 (72/72)	Pulmonary nodule	Seventy–two normal PA CXR were duplicated, used to generate an experimental data. Nodules ranging in size from 8 to 12 mm were superimposed on each radiograph. The nodules (total of 119) were evenly and randomly distributed among the 432 possible regions	Any pulmonary or pleural abnormality including nodules, incomplete inclusion of the thorax in the field of view, reduced lung volumes, and overlying devices or markers	Normal PA CXR were selected retrospectively from routine adult outpatient clinical case loads	CXR Six readers: 3 experts (with 22 y experience), 3 less experienced radiologists (4 y)	Radiologist	Simulated nodules
Robinson et al. (2013/ Australia)	30 (15/15)	Pulmonary nodule	A single digitally imposed lesion with diffuse edge and a Gaussian contrast profile of varying subtlety and measuring between 6 and 12 mm in diameter, was subsequently inserted on each of 15 images	–	–	CXR Sixteen examining radiologists with ABR and 21 y expertise	Expert thoracic radiologist	–
Kirchner et al. (2013/ Germany)	55 (47/8)	Pulmonary nodule	Cases presenting small single pulmonary nodules ranging from 6–12 mm. This review was performed by means of a retrospective computer–aided analysis of all CT scans (in total 3831). From these examinations the study leader selected 47 cases in which the presence and location of a single small (6–12 mm), non– calcified peripheral nodule could, in retrospect, be confirmed on corresponding conventional PA CXR	Nodule size greater than 12 mm. Some small nodules in the central parts of the lung were excluded	–	CXR Five radiologists: • Group A: 2 very experienced readers in thoracic radiology (board certified radiologists) • Group B: 3 less experienced readers	Chest CT scan	–
Park et al. (2014/South Korea)	110 (55/55)	Rib Fx	–	Prominent Fx detected by a 1st grade medical student and 67 cases with associated injuries including, but not limited to hemothorax, PTX, pulmonary contusion, and subcutaneous emphysema, which are more likely to imply rib Fx	–	CXR Twenty readers: 5 junior and 5 senior EM residents, 10 fourth year medical students	Experienced chest radiologist	–

Copyright © 2023 Tehran University of Medical Sciences
This work is licensed under a Creative Commons Attribution-NonCommercial 4.0 International license (https://creativecommons.org /licenses/by-nc/4.0/).
Noncommercial uses of the work are permitted, provided the original work is properly cited.

Table 1 Included studies characteristics (continued)

Study (Y/C)	Sample size (case/ control)	Type of disease	Inclusion criteria	Exclusion criteria	Control group	Index test reader(s)	Reference test(s)	Comment(s)
Thompson et al. (2016/UK)	75 (50/25)	Pulmonary nodule	PA images of an anthropomorphic chest phantom which was loaded with spherical nodules of 5, 8, 10 and 12 mm diameter and of 100–Hounsfield unit contrast that distributed evenly within the lung fields. Fifty different configurations of nodule positions were simulated and each nodule size could appear only once in each case. Each configuration of nodules represented a single case. Abnormal cases contained 1–4 nodules	–	–	CXR Six consultant radiologists with 5–32 y experience	Radiologist	–
Musalar et al. (2017/Turkey)	268 (106/162)	PTX	PA CXR of patients>18 y, diagnosed with PTX in ER and a stratified random sample of patients who presented with chest pain and breathlessness, yet were not found to have PTX	Inadequacy of the records and PACS images inappropriate for radiological evaluation. Ten patients with diagnosis of occult PTX	–	CXR Ten assistant researchers EM specialists with at least 3 y experience of specialization who indicated that they had used inverted gray–scale PACS during diagnostic process of PTX assumed tasks in the study	Radiologist	–
Boyd et al. (2020/US)	52 (26/26)	ELVO	–	Positive studies beyond middle cerebral artery main stem	By querying the PACS, and were confirmed as negative prior to any reading sessions by consensus review by 2 experienced interventional neuroradiologists	Brain CTA Eighteen readers: 2 faculty interventional neuroradiologists, 2 faculty diagnostic neuroradiologists, 10 faculty radiologists who all interpret stroke CTA but without formal neuroradiology fellowship training, and 4 radiology residents	Two interventional neuroradiologists positive CTAs confirm with conventional angiography	–

Copyright © 2023 Tehran University of Medical Sciences
This work is licensed under a Creative Commons Attribution-NonCommercial 4.0 International license (https://creativecommons.org /licenses/by-nc/4.0/).
Noncommercial uses of the work are permitted, provided the original work is properly cited.

Table 1 Included studies characteristics (continued)

Study (Y/C)	Sample size (case/ control)	Type of disease	Inclusion criteria	Exclusion criteria	Control group	Index test reader(s)	Reference test(s)	Comment(s)
Eken et al. (2021/ Turkey)	60	Tibia pilon Fx	Patients admitted for orthopaedic trauma association foundation type C3 pilon Fx between January 2018 and June 2020, who were skeletally mature (≥18 y) at the date of admission and available plain radiographs and CT scan images after ankle spanning external fixator applied	Open Fx, previous ankle surgery and inadequate radiological records	–	AP and lateral view of ankle in traction were interpreted by 20 observers (5 orthopedic trauma surgeons, 10 general orthopedic surgeons, and 5 radiologist)	CT scans were from 5 cm above the ankle joint to the subtalar joint	CT scans were obtained before skeletal traction application, at the emergency service
Patel et al. (2021/UK)	50 28/50: fusion abnormality, 14/50: hardware loosening, 8/50: hardware Fx	Presence of fusion, Fx and loosening of spinal implant	Patients>18 y from our spinal orthopedic database who had history of spinal surgery with implant insertion and underwent postoperative CT scan imaging as part of their spinal orthopedic hardware follow up.	–	–	Two radiologists and 1 orthopedic surgeon independently reviewed all the images. One of the radiologists had approximately 7 y experience in reviewing post–operative CT scans, the other was at the end of a musculoskeletal fellowship program and had 3 y experience in reviewing post–operative CT scans and the orthopedic surgeon had 6 y experience in reviewing post–operative CT scans.	The review of the entire data set for the study, along with any previous and subsequent CT scans, radiographs and the patients' clinical picture in a multidisciplinary setting attended by a consultant radiologist (senior author of the study) and the orthopedic surgeon who had overall clinical responsibility for the patient.	All images reviewed twice over 2 separate reading sessions 2 m apart, one session viewed on the conventional CT scan, bone windows and the other session was viewed with greyscale inversion.

Copyright © 2023 Tehran University of Medical Sciences
This work is licensed under a Creative Commons Attribution-NonCommercial 4.0 International license (https://creativecommons.org /licenses/by-nc/4.0/). Noncommercial uses of the work are permitted, provided the original work is properly cited.

Table 1 Included studies characteristics (continued)

Study (Y/C)	Sample size (case/ control)	Type of disease	Inclusion criteria	Exclusion criteria	Control group	Index test reader(s)	Reference test(s)	Comment(s)
Ledda et al. (2022/Italy)	**507 atelectasis 166/507) Consolidation (175/507) ILD (67/507) nodule (85/507) Mass (10/507) Pleural effusion (167/507) PTX (28/507) Rib Fx (65/507)	Atelectasis, consolidation, ILD, nodule, mass, pleural effusion, PTX and rib Fx .	Patients who underwent a chest CT scan examination and a CXR within 24 h were enrolled	CT scan and CXR images affected by motion artefacts or other technical limitations (e.g., chest structures only partially included within the CT scan acquisition volume or the CXR projection) were excluded	–	CXR One general radiologist with 18 y of experience (reader 1), two 3^{rd}–y radiology residents (readers 2 and 3)	Chest CT scan images were reviewed independently by two resident radiologists (readers 4 and 5, respectively) who had access to the radiological reports. Any discrepancy between readers 4 and 5 was resolved by a chest radiologist with 13 y of experience.	–

* Readers in index test and reference test are separated until mentioned otherwise
**Some patients had more than one lesion
Y/C: Year/country; CXR: Chest X-ray; Y: Years; PTX: Pneumothorax; Fx: Fracture; ILD: Interstitial lung disease; m: Months; ER: Emergency room; PA: Posteroanterior; ABR: American board of radiology; EM: Emergency medicine; PACS: Picture archiving communication system;
ELVO: Emergent large vessel occlusions; CTA: Computed tomo angiography; OTA: Orthopedic trauma association;
AP: Anteroposterior; h: Hours; mm: Millimeter; cm: Centimeter

Table 2 Risk of bias

Author (year/ country)	Bias				Applicability		
	Patient selection	Index test	Reference standard	Flow and timing	Patient selection	Index test	Reference standard
Oestmann et al. (1987/US)	L	L	L	L	L	L	L
MacMahon et al. (1987/US)	L	L	L	L	L	L	L
Sheline et al. (1988/US)	L	U	L	L	L	L	L
Oestmann et al. (1989/US)	L	L	L	L	L	L	L
KheddacheS et al. (1991/Sweden)	L	L	L	L	L	L	L
Kehler et al. (1991/Sweden)	L	L	L	L	L	L	L
Schaefer et al. (1991/US)	U	L	L	L	H	L	L
Buckley1 et al. (1991/US)	L	L	L	L	L	L	L
Choi et al. (2002/Korea)	L	L	L	L	L	L	L
KANG et al. (2004/South Korea)	L	L	L	U	L	L	L
De Boo et al. (2011/The Netherlands)	L	L	L	L	L	L	L
Lungren et al. (2011/US)	L	L	L	L	L	L	L
Robinson et al. (2013/Australia)	L	L	L	L	L	L	L
Kirchner et al. (2013/Germany)	U	L	L	L	H	L	L
Park et al. (2014/South Korea)	L	L	L	L	L	L	L
Thompson et al. (2016/UK)	L	L	L	L	L	L	L
Musalar et al. (2017/Turkey)	L	L	L	L	L	L	L
Boyd et al. (2020/US)	L	L	L	U	L	L	L
Eken et al. (2021/Turkey)	H	L	L	L	L	L	L
Patel et al. (2021/UK)	L	L	L	L	L	L	L
Ledda et al. (2022/Italy)	L	L	L	L	L	L	L
Sum 21	L:18 U: 2 H: 1	L: 20 U: 0 H: 0	L: 21 U: 0 H: 0	L: 19 U: 2 H: 0	L: 19 U: 0 H: 2	L: 21 U: 0 H: 0	L: 21 U: 0 H: 0

L: Low; U: Unclear; H: High

Copyright © 2023 Tehran University of Medical Sciences
This work is licensed under a Creative Commons Attribution-NonCommercial 4.0 International license (https://creativecommons.org /licenses/by-nc/4.0/). Noncommercial uses of the work are permitted, provided the original work is properly cited.

Table 3 Study performances on pulmonary nodule

Study		Conventional mode							Applicability							Combined mode[a]
		Sensitivity (95% CI)	Specificity (95% CI)	NPV	PPV	LR–	LR+	Accuracy (95% CI)	Sensitivity (95% CI)	Specificity (95% CI)	NPV	PPV	LR–	LR+	Accuracy (95% CI)	–
Oestmann et al. (1987/US)		0.71	0.95[b]	–	–	0.30[χ]	14.2[b]	0.83	0.57	0.91[b]	–	–	0.47[b]	6.33[b]	0.74	–
MacMahon et al. (1987/US)	PTX	–	–	–	–	–	–	Equal	–	–	–	–	–	–	Equal	–
	Bone lesion	–	–	–	–	–	–	Superior	–	–	–	–	–	–	Inferior	–
	Infiltration		–	–	–	–	–	Superior	–	–	–	–	–	–	Inferior	–
	Nodule		–	–	–	–	–	Superior	–	–	–	–	–	–	Inferior	–
	Overall		–	–	–	–	–	Superior	–	–	–	–	–	–	Inferior	–
Oestmann et al. (1988/US)		–	–	–	–	–	–	0.87 (0.86–0.88 [c])[b]	–	–	–	–	–	–	0.87 (0.86–0.88 [d])[b]	–
Sheline et al. (1988/ US)		–	–	–	–	–	–	0.75 (0.69–0.81[e])[b]	–	–	–	–	–	–	0.86 (0.74–0.98[f])[b]	–
Kheddache S et al. (1991/ Sweden)	Small nodule w/o edge enhancement variable light	–	–	–	–	–	–	0.73[g]	–	–	–	–	–	–	0.75[g]	–
	Large nodule w/o edge enhancement variable light	–	–	–	–	–	–	–	0.66[g]	–	–	–	–	–	0.75[g]	–
	PTX with edge enhancement	–	–	–	–	–	–	0.90	–	–	–	–	–	–	0.92	–
Kehler et al. (1991/ Sweden)	All lung regions	–	–	–	–	–	–	0.75	–	–	–	–	–	–	0.83	–
	Behind mediastinum	–	–	–	–	–	–	0.96	–	–	–	–	–	–	0.90	–

Copyright © 2023 Tehran University of Medical Sciences
This work is licensed under a Creative Commons Attribution-NonCommercial 4.0 International license (https://creativecommons.org /licenses/by-nc/4.0/).
Noncommercial uses of the work are permitted, provided the original work is properly cited.

Table 3 Study performances on pulmonary nodule (continued)

Study		Conventional mode							Applicability							Combined mode[a]
		Sensitivity (95% CI)	**Specificity (95% CI)**	**NPV**	**PPV**	**LR–**	**LR+**	**Accuracy (95% CI)**	**Sensitivity (95% CI)**	**Specificity (95% CI)**	**NPV**	**PPV**	**LR–**	**LR+**	**Accuracy (95% CI)**	–
Choi et al. (2002/ Korea)		–	–	–	–	–	–	0.86 (0.80–0.92)[hbg]	–	–	–	–	–	–	0.81 (0.66–0.96)[ibg]	0.88 (0.87–0.90)[jbg]
De Boo et al. (2011/ The Netherlands)	All experiences	0.48 (0.45-0.52)	–	–	–	–	–	–	–	–	–	–	–	–	–	Sensitivity: 0.50 (0.46–0.54)
	Experienced	0.55 (0.49–0.59)	–	–	–	–	–	0.77 (0.73–0.82)	–	–	–	–	–	–	–	Sensitivity: 0.55 (0.50–0.60)
	Inexperienced	0.42 (0.37–0.47)	–	–	–	–	–	0.66 (0.61–0.71)	–	–	–	–	–	–	–	Sensitivity: 0.45 (0.40–0.50)
Lungren et al. (2011/US)		0.78 (0.73–0.84)[g]	0.5 (0.83–0.87)[g]	–	–	0.26 [b]	4.33[b]	Unobscured lung regions: 0.87 (0.78–0.95)[g] Obscured lung regions[k]: 0.78 (0.72–0.84)	0.60 (0.54–0.67)[g]	0.89 (0.87–0.91)[g]	–	–	0.44[b]	5.45[b]	Unobscured lung regions: 0.75 (0.70–0.81)[g] Obscured lung regions: 0.78 (0.73–0.83)	Sensitivity: 0.69 (0.63–0.75)[g] Specificity: 0.89 (0.87–0.91)[g] LR–: 0.34[b] LR+: 6.27[b] Unobscured lung regions AUC: 0.79 (0.72–0.86)[g] Obscured lung regions: 0.80 (0.73–0.87)
Robinson et al. (2013/ Australia)		–	–	–	–	–	–	0.71 (0.63–0.76)[g]	–	–	–	–	–	–	0.76 (0.71–0.80)[g]	–
Kirchner et al. (2013/ Germany)	All experienced	0.57 (0.50–0.63)[g]	0.73 (0.57–0.86)[g]	0.25[Σ]	0.91[Σ]	0.60[Σ]	2.06Σ	0.69[Σ]	0.63 (0.57–0.69)[g]	0.75 (0.59–0.87)[g]	0.29Σ	0.93Σ	0.40[Σ]	2.01[Σ]	0.81[Σ]	–

Copyright © 2023 Tehran University of Medical Sciences
This work is licensed under a Creative Commons Attribution-NonCommercial 4.0 International license (https://creativecommons.org /licenses/by-nc/4.0/). Noncommercial uses of the work are permitted, provided the original work is properly cited.

Table 3 Study performances on pulmonary nodule (continued)

Study		Conventional mode							Applicability							Combined mode[a]
		Sensitivity (95% CI)	**Specificity (95% CI)**	**NPV**	**PPV**	**LR–**	**LR+**	**Accuracy (95% CI)**	**Sensitivity (95% CI)**	**Specificity (95% CI)**	**NPV**	**PPV**	**LR–**	**LR+**	**Accuracy (95% CI)**	–
	Experienced	0.59 (0.49–0.68)	0.41 (0.32–0.51)	0.17	0.83	1.00	1.00	0.72[g] (0.62–0.80)[g]	0.72 (0.63–0.81)	0.88 (0.62–0.98)	0.39	0.97	0.32	5.77	0.91[g] (0.84–0.96)[g]	–
	Less experienced	0.59 (0.49–0.68)	0.41 (0.32–0.51)	0.29	0.96	0.50	4.51	0.79 (0.70–0.86)	0.72 (0.63–0.81)	0.88 (0.62–0.98)	0.24	0.89	0.65	1.69	0.70 (0.61–0.79)	–
Thompson et al. (2016/ UK)		0.71	0.84	–	–	0.34 b	4.43[b]	0.75[b]	0.75	0.74	–	–	0.33 b	2.88[b]	0.74[b]	–

CI: Confidence interval; NPV: Negative predictive value; NL–: Negative likelihood ratio; PPV: Positive predictive value; PL+: Positive likelihood ratio; PTX: Pneumothorax; W/O: without; a: Conventional and inverse modes used simultaneously; b: For parameters not reported in study texts manual calculation was performed if possible; c: Calculated from mean ± standard deviation (0.87±0.05); d: Calculated from mean ± standard deviation (0.87±0.03); e: Calculated from mean ± standard error (0.75±0.06); f: Calculated from mean ± standard error (0.86±0.06); g: Parameters with significant difference; h: Calculated from mean ± standard deviation (0.8893±0.0297); i: Inverse mode performance was significantly lower from the other modes/calculated from mean±standard deviation (0.8095 ± 0.0743); j: Calculated from mean ± standard deviation (0.8835 ± 0.0660); k: Behind the heart/mediastinum and diaphragms

Four studies evaluated pneumothorax (PTX) in inverse mode (41,42) and among them, the only significant change in performance was found in Musalar et al. where the inverse mode showed lower sensitivity (42). Of note, the combined mode is used in one study (40) (Table 3).

Eight studies used the inverse mode for other lesions and found significant improvements in test performances. Both of studies on orthopedic lesions indicated better performance in some aspects: a study on pilon fractures by Eken et al. showed better accuracy for the inverse mode when evaluating posterolateral fragment and the lateral zone of comminution (35). The other, investigated the images of spinal devices during the follow–up period and the sensitivity for evaluating the fusion and loosening of the devices was increased (43). One study on bullous lung disease showed lower accuracy (44). Meanwhile Schaefer et al. showed higher specificity, lower sensitivity, and lower accuracy for ILDs (37). Four of these eight studies evaluated the combined mode. In contrast to the studies on inverse mode, none of these studies indicated a lower performance. In fact, Kang et al. study on urinary calculus demonstrated better accuracy (29), one study on rib fracture (5) indicated better sensitivity and the remaining showed insignificant differences. Image interpretation in all these studies was performed by practitioners with various experiences (Table 4).

Two studies on pulmonary nodule (30,39), with a total of 199 cases, showed higher inverse mode specificity (0.8, 95% CI: 0.70,0.92) and lower sensitivity (0.68, 95% CI: 0.47,0.88) in comparison to conventional mode. Heterogeneity for conventional mode sensitivity was significant (P=0.00) (Table 5).

In meta–analysis of AUC of 250 cases in four studies on pulmonary nodules (28,33,34,38), inverse mode showed improved accuracy (0.83, 95% CI: 0.75,0.90) in comparison with conventional mode (0.80, 95% CI: 0.72,0.88) (Table 5) (Figures 2–4).

4. Discussion

Our study showed that application of inverse mode when using radiography for detection of pulmonary nodules may improve the diagnostic accuracy. Although inverse/combined mode demonstrated better performance for other lesions in some studies, the results were insignificant.

4.1. Pulmonary nodule

Meta–analysis revealed that the inverse mode is more accurate than the conventional mode in detecting pulmonary nodules. However, the recommendation (GRADE) was rated as very low due to study limitations. Moreover, practitioners can take the most advantage of the combined mode where they can detect the lesions using the more sensitive conventional mode and then confirm its presence through application of the more specific inverse mode. However, neither inverse nor combined mode application resulted in negative likelihood ratio (LR–)<0.1 and positive likelihood ratio (LR+)>10; figures which are meaningful from a clinical standpoint (45). Similarly, there was only one study in which AUC of using inverse mode was ≥0.7 (39,46). To compare performance of the combined mode with the inverse mode, we found only one study that showed readers performance was increased with the former while decreased with the latter (28).

The other studies demonstrated significantly better perfor-

Copyright © 2023 Tehran University of Medical Sciences
This work is licensed under a Creative Commons Attribution-NonCommercial 4.0 International license (https://creativecommons.org /licenses/by-nc/4.0/). Noncommercial uses of the work are permitted, provided the original work is properly cited.

Table 4 Study performances on other lesions

Study		**Conventional mode**					**Inverse mode**					**Combined mode**
		Sensitivity (95% CI$^{\alpha}$)/N	**Specificity (95% CI)/N**	**LR–**	**LR+**	**Accuracy (95% CI)**	**Sensitivity (95% CI)**	**Specificity (95% CI)**	**LR–**	**LR+**	**Accuracy (95% CI)**	–
Schaefer et al. (1991/US)		0.78$^{\Sigma}$ (0.75–0.81)$^{\chi,¶}$	0.70 (0.63–0.77)$^{¶¶\chi\Sigma}$	0.31 $\chi\Sigma$	2.60 $\chi\Sigma$	0.88 (0.87–0.89)¶¶¶ $\chi\Sigma$	0.52 (0.49–0.55)$^{\Omega\chi\Sigma}$	0.85 (0.82–0.88)$^{\Omega\Omega}$ $\chi\Sigma$	0.56$^{\chi}$ Σ	3.4$^{\chi}\Sigma$	0.83(0.81– –0.85)$^{\Omega\Omega}$ $\Omega\Sigma\chi$	–
Buckley1 et al. (1991/US)		–	–	–	–	0.76 (0.64–0.87)$^{\Sigma}$	–	–	–	–	0.60 (0.37–0.72)$^{\Sigma}$	–
KANG et al. (2004 /South Korea) The performance of all observers for all urinary stone locations		–	–	–	–	0.66$^{\Sigma}$	–	–	–	–	0.720	0.76$^{\Sigma}$
Park et al. (2014/ South Korea)	All experiences	0.60 1666/ 2780	0.85 937/1100	0.47 χ	4.00 χ	0.67 2603/ 3880	0.60 1684/ 2780	0.86 940/ 1100	0.46$^{\chi}$	4.28$^{\chi}$	0.68 2624/ 3880	Sensitivity: 0.65$^{\Sigma}$ 1806/ 2780 Specificity: 0.86 947/ 1100 Accuracy: 0.71 2753/ 3880 LR-: 0.40 LR+: 4.64
	All residents	0.61 852/1390	0.89 491/550	0.43 χ	5.54 χ	0.69 1342/1940	0.60 840/1390	0.89 489/550	0.44 $^{\chi}$	5.45 $^{\chi}$	0.69 1328/1940	Sensitivity: 0.65$^{\Sigma}$ 909/ 1390 Specificity: 0.88 482/550 Accuracy: 0.72 1391/1940
	Senior residents	0.65 451/695	0.94 258/275	0.37 χ	10.83 χ	0.73 709/970	0.61 423/695	0.92 254/275	0.42 $^{\chi}$	7.62 $^{\chi}$	0.70 677/970	Sensitivity: 0.62 428/695 Specificity: 0.98 268/275 Accuracy: 0.72 696/970
	Junior residents	0.58 401/695	0.85 233/275	0.49 χ	3.86 χ	0.65 634/970	0.60 416/695	0.86 235/275	0.46 $^{\chi}$	4.28 $^{\chi}$	0.67 651/970	Sensitivity: 0.69$^{\Sigma}$ Specificity: 0.78 214/275 Accuracy: 0.72$^{\Sigma}$
	All students	0.59 814/1390	0.81 446/550	0.50 χ	3.10 χ	0.65 1260/1940	0.61 845/1390	0.82 451/550	0.47 $^{\chi}$	3.38 $^{\chi}$	0.67 1296/1940	Sensitivity: 0.65$^{\Sigma}$ 897/1390 Specificity: 0.85 465/550 Accuracy: 0.70$^{\Sigma}$ 1362/ 1940
Musalar et al. (2017/ Turkey)		0.92 (0.89–0.94)$^{\Sigma}$ 486/ 530	0.96 (0.94–0.97) 778/ 810	23.21 (16.51 -32.63)	0.09 (0.07-0.1 1)	0.94 (0.92-0.95) 1264/ 1340	0.85 (0.81–0.88) $^{\Sigma}$ 448/530	0.97 (0.96–0.98) 789/ 810	32.60 (21.34–49.81)	0.16 (0.13–0.19)	0.91 (0.89–0.92) 1237/1340	–

Copyright © 2023 Tehran University of Medical Sciences
This work is licensed under a Creative Commons Attribution-NonCommercial 4.0 International license (https://creativecommons.org /licenses/by-nc/4.0/). Noncommercial uses of the work are permitted, provided the original work is properly cited.

Table 4 Study performances on other lesions (continued)

Study		Conventional mode					Inverse mode					Combined mode
		Sensitivity (95% CI$^{\alpha}$)/N	Specificity (95% CI)/N	LR–	LR+	Accuracy (95% CI)	Sensitivity (95% CI)	Specificity (95% CI)	LR–	LR+	Accuracy (95% CI)	–
Boyd et al. (2020/ US)	Overall	0.96 (0.92–0.98)	0.97 (0.94–0.98)	0.04 $^{\chi}$	32 $^{\chi}$	0.96 (0.94–0.98)	0.97 (0.93–0.99)	0.97 (0.94–0.99)	0.03$^{\chi}$	32.33 $^{\chi}$	0.97 (0.95–0.98)	–
	Neurora–diology	0.94 (0.87–0.97)	0.97 (0.91–0.99)	0.06 $^{\chi}$	31.33 $^{\chi}$	0.95 (0.91–0.97)	0.96 (0.91–0.99)	0.99 (0.96–1.00)	0.04$^{\chi}$	96$^{\chi}$	0.97 (0.95–0.99)	–
	Non–neurora–diology	0.97 (0.93–0.99)	0.97 (0.95–0.99)	0.03 $^{\chi}$	32.33 $^{\chi}$	0.97 (0.95–0.98)	0.98 (0.95–0.99)	0.97 (0.93–0.99)	0.02$^{\chi}$	32.66 $^{\chi}$	0.98 (0.95–0.99)	–
	Resident	0.95 (0.90–0.98)	0.96 (0.91–0.98)	0.05 $^{\chi}$	23.75 $^{\chi}$	0.96 (0.92–0.97)	0.94 (0.87–0.98)	0.96 (0.92–0.98)	0.06$^{\chi}$	23.50 $^{\chi}$	0.95 (0.91–0.97)	–
Eken et al. (2021/ Turkey)	Fragment Medial malleolus						0.5				0.47	
	Anterolateral						0.72				0.8	
	Posterolateral						0.62				0.77$^{\Sigma}$	
	Zone of comminution Lateral						0.58				0.7$^{\Sigma}$	
	Central						0.75				0.77	
	Medial shoulder						0.45				0.46	
Patel et al. (2021/ UK)	Fusion	0.7	0.89	–	–	–		0.83$^{\Sigma}$	0.79	–	–	–
	Loosening		0.74	1	–	–	–	0.9$^{\Sigma}$	0.67	–	–	–
	Fracture		1	1	–	–	–	1	1	–	–	–
Ledda et al. (2022/ Italy)		0.07–0.6	0.76–0.99	–	–	0.53–0.78	0.08–0.6	0.78–0.99	–	–	0.53–0.78	First conventional mode then inverse mode: Sensitivity: 0.08–0.6 Specificity: 0.73–1 AUC: 0.53–0.78 First inverse mode then conventional mode: Sensitivity: 0.08–0.6 Specificity: 0.73–1 AUC: 0.53–0.78

CI: Confidence interval; LR–: Negative likelihood ratio; LR+: Positive likelihood ratio;
¶: Calculated from mean ± standard error (0.78±0.03); ¶¶: Calculated from mean ± standard error (0.70±0.07);
¶¶¶: Calculated from mean ± standard error (0.88±0.01); Ω: Calculated from mean ± standard error (0.52 ± 0.03);
Ω Ω: Calculated from mean ± standard error (0.85 ± 0.03); Ω Ω Ω: Calculated from mean ± standard error (0.83±0.02);
χ: For parameters not reported in study texts, manual calculation was performed, if possible;
Σ: Parameters with significant difference

Copyright © 2023 Tehran University of Medical Sciences
This work is licensed under a Creative Commons Attribution-NonCommercial 4.0 International license (https://creativecommons.org /licenses/by-nc/4.0/).
Noncommercial uses of the work are permitted, provided the original work is properly cited.

Table 5 Pooled indices for conventional and inverse modes and corresponding heterogeneities in the meta-analysis

	Sensitivity (Confidence interval 95%)			Specificity (Confidence interval 95%)			Area under curve (Confidence interval 95%)		
Conventional mode	0.68 (0.47–0.88)	Q–squared	23.37	0.81 (0.70–0.92)	Q–squared	2.58	0.80 (0.72–0.88)	Q–squared	38.23
		P–value	0.00		P–value	0.11		P–value	0.00
		I^2	95.7%		I^2	61.3%		I^2	92.2%
		Tau–squared	0.0211		Tau–squared	0.0044		Tau–squared	0.0059
Inverse mode	0.62 (0.57–0.66)	Q–squared	0.44	0.84 (0.71–0.97)	Q–squared	3.76	0.83 (0.75–0.90)	Q–squared	22.39
		P–value	0.50		P–value	0.52		P–value	0.00
		I^2	0.0%		I^2	73.4%		I^2	86.6%
		Tau–squared	0.0000		Tau–squared	0.0072		Tau–squared	0.0044

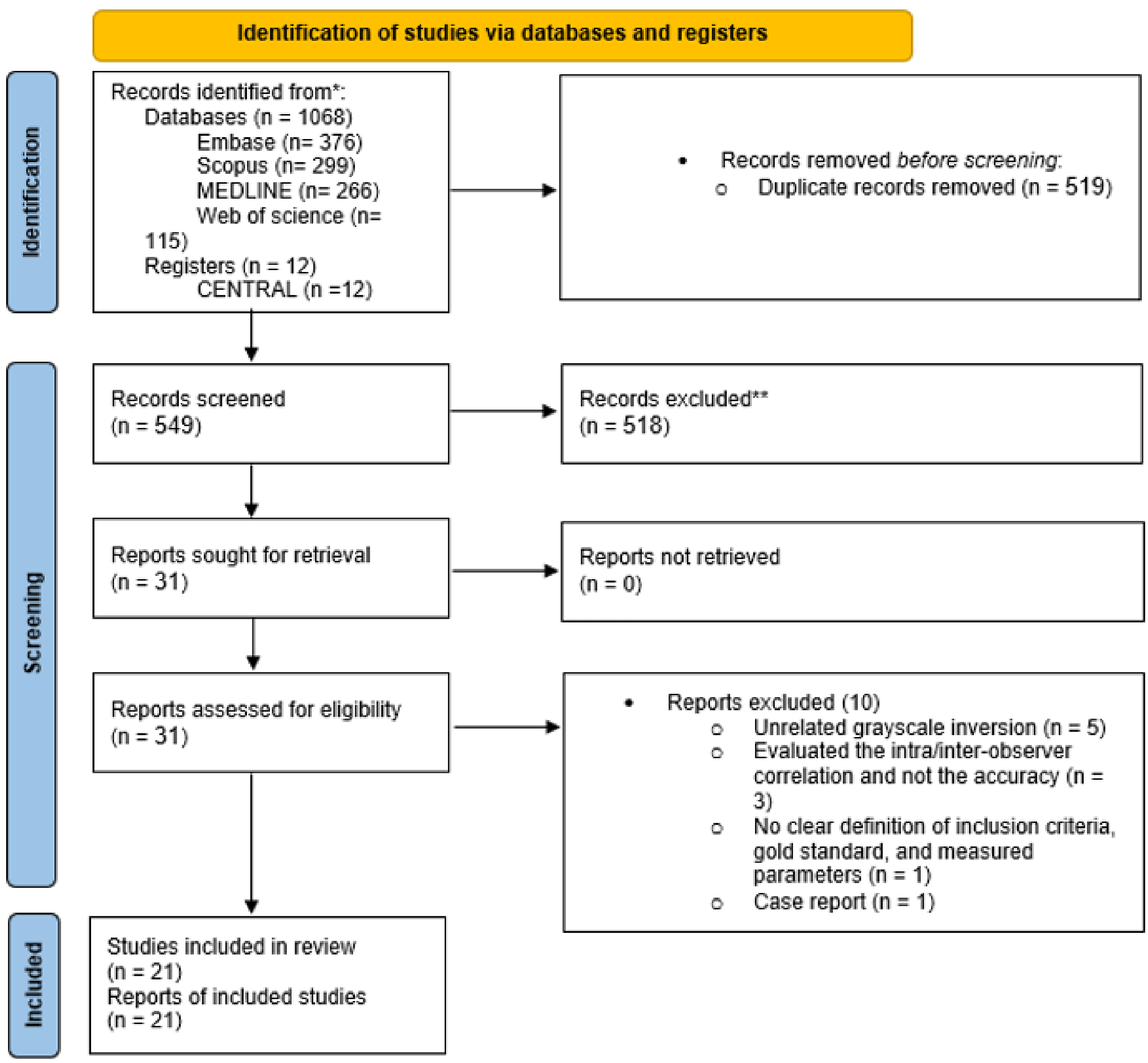

Figure 1 The flowchart illustrates study selection criteria and the results

Copyright © 2023 Tehran University of Medical Sciences
This work is licensed under a Creative Commons Attribution-NonCommercial 4.0 International license (https://creativecommons.org /licenses/by-nc/4.0/). Noncommercial uses of the work are permitted, provided the original work is properly cited.

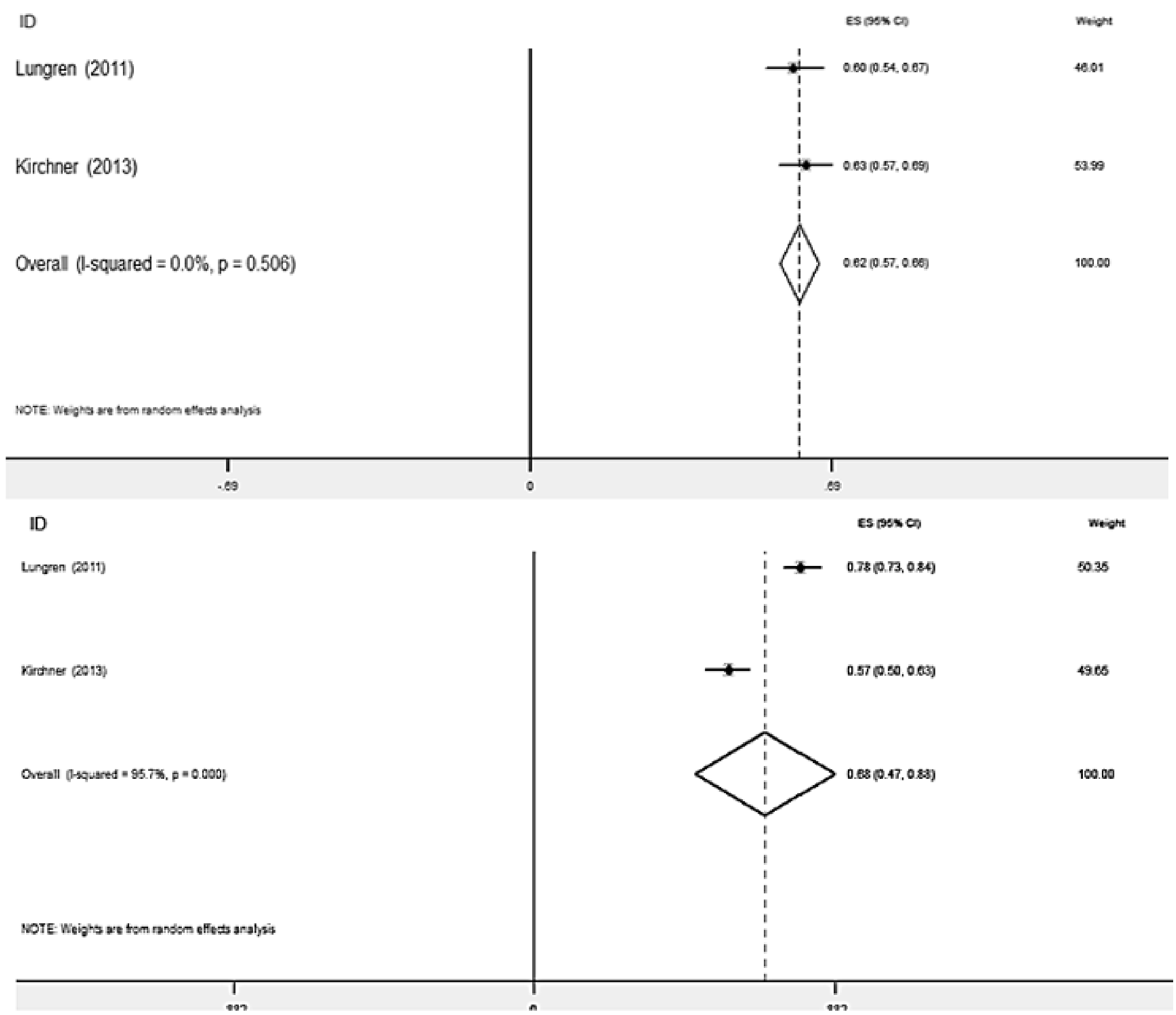

Figure 2 Conventional (below) and inverse mode (above) sensitivity forest plot

mance of both combined and inverse mode in comparison with the conventional mode (28–30). The subjective preference of readers for choosing between the conventional and inverse mode is asked in one study which was similar (41).

4.2. Other abnormalities

Investigated lesions in the emergency department were PTX, urinary calculus, rib fracture, and ELVO. Among four studies evaluating PTX by inverse mode, Musalar et al. showed lower sensitivity and higher specificity (42) (Table 4). It would be difficult to include the other three studies in reaching a conclusion on PTX, since the observed improved accuracy in Kheddache et al. is confounded by applying edge enhancement simultaneous with inverse mode (32), MacMahon et al. reported results in a semi quantitative manner (41), and the other one analyzed the readers performances in separate groups (40).

One study evaluating urinary calculus (29) showed that abdominal radiograph interpretation in either the inverse mode or the combined mode increased accuracy in comparison with the conventional mode. When asked which modality clinician preferred to use, combined mode received the highest degree of subjective preference. Limitations of this study include the possibility of calculus migration before performing the gold standard tests and also, including equal proportions of each urinary calculi location in contrast with the real prevalence.

The two studies on rib fracture failed to show any significant difference between the inverse and conventional modes (5,40).

However, Park et al. demonstrated the combined mode resulted in improved performance of less experienced readers (junior residents and medical students) when detecting subtle fractures (5).

To evaluate the accuracy of all three modes in chest X–ray (CXR) for all clinically important lesions, Ledda et al. reported no significant difference among modes for expert radiologists but the combined mode resulted in reduced interobserver variability in readers with limited expertise (40).

There were two studies in the literature that investigated

Copyright © 2023 Tehran University of Medical Sciences
This work is licensed under a Creative Commons Attribution-NonCommercial 4.0 International license (https://creativecommons.org /licenses/by-nc/4.0/). Noncommercial uses of the work are permitted, provided the original work is properly cited.

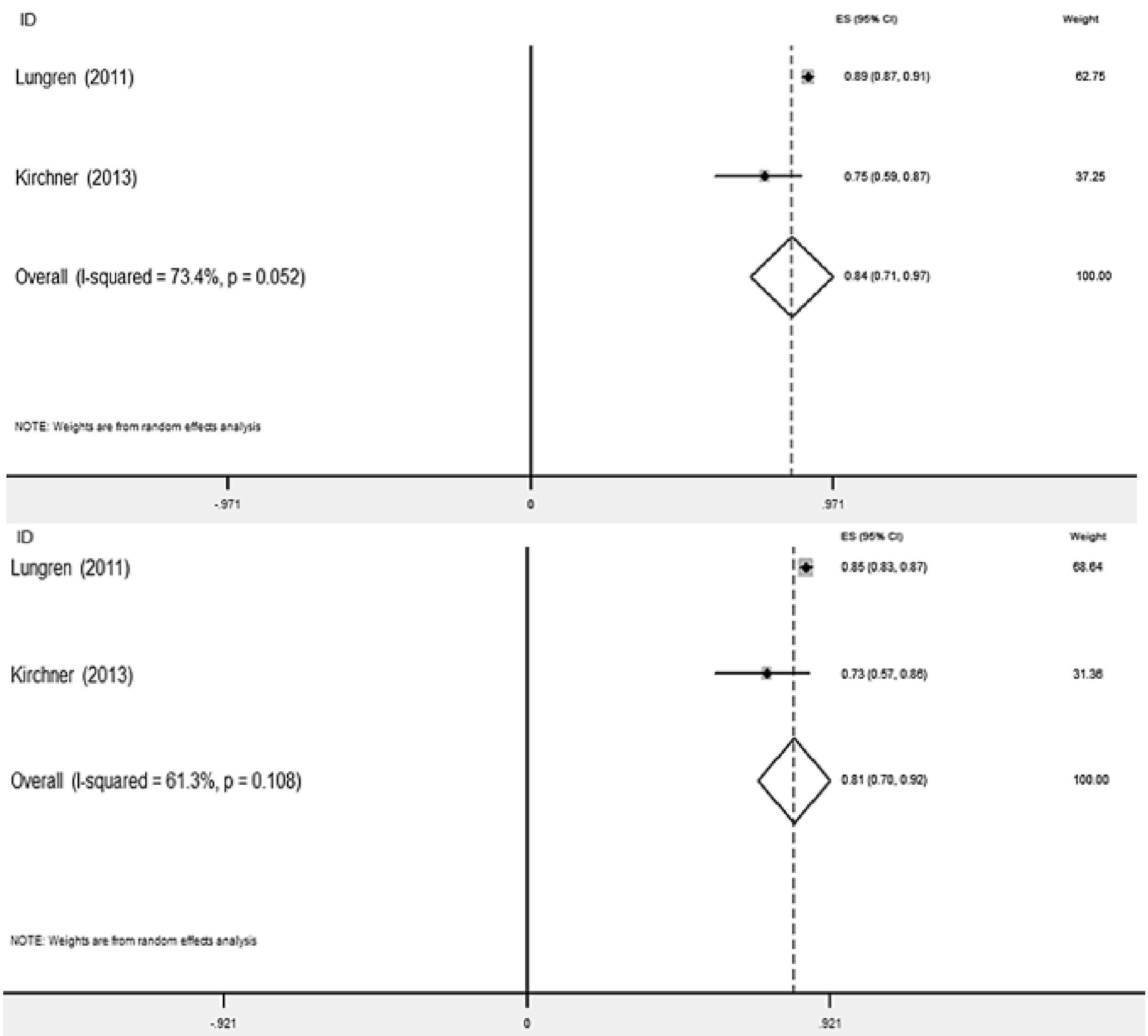

Figure 3 Conventional (below) and inverse mode (above) specificity forest plot

grayscale inversion in computed tomography (CT) scan (43,47). Boyd et al. investigated the diagnosis of ELVO by clinicians of various experience in a single center and showed no significant improvement in accuracy after inverse mode application (47). However, brain computed tomography angiography (CTA) in both modes had equally high accuracy of about 97 percent. Another study looked at post–operative spinal implants and demonstrated better inverse mode sensitivity for evaluating the fusion and loosening of devices (43).

4.3. Factors with possible influence on accuracy

Some studies included factors with potential influence on accuracy: different readers experience (4,5,31,39,47), reading time limit (29,33,36,41), edge enhancement (31–33, 36,37,44), permission to change settings (e.g. light and contrast) (4,5,28,30–34,38,39,42), and lesions in obscured lung areas (e.g. mediastinum, diaphragm) (30,31,34). Owing to insufficient investigations, we cannot draw any firm conclusions regarding the possible effect of these factors.

The familiarity with the inverse mode is an important aspect that has been noted in almost all studies. Previous experience can have an effect on observer performance in either of the following two ways. Experienced personnel may have better performance using the inverse mode as they possess more experience with similar utilities such as chest fluoroscopy (39). Experience can also prove to be a hinderance as individuals more familiar with the conventional method may be reluctant to rely on the new image setting (5,34,40).

In addition, eight studies (31–33,36–38,41,44) used old image processing technologies which might have negatively impacted the quality of images. This probably contributed to the inconsistency of the results (1,37,39).

Copyright © 2023 Tehran University of Medical Sciences
This work is licensed under a Creative Commons Attribution-NonCommercial 4.0 International license (https://creativecommons.org /licenses/by-nc/4.0/). Noncommercial uses of the work are permitted, provided the original work is properly cited.

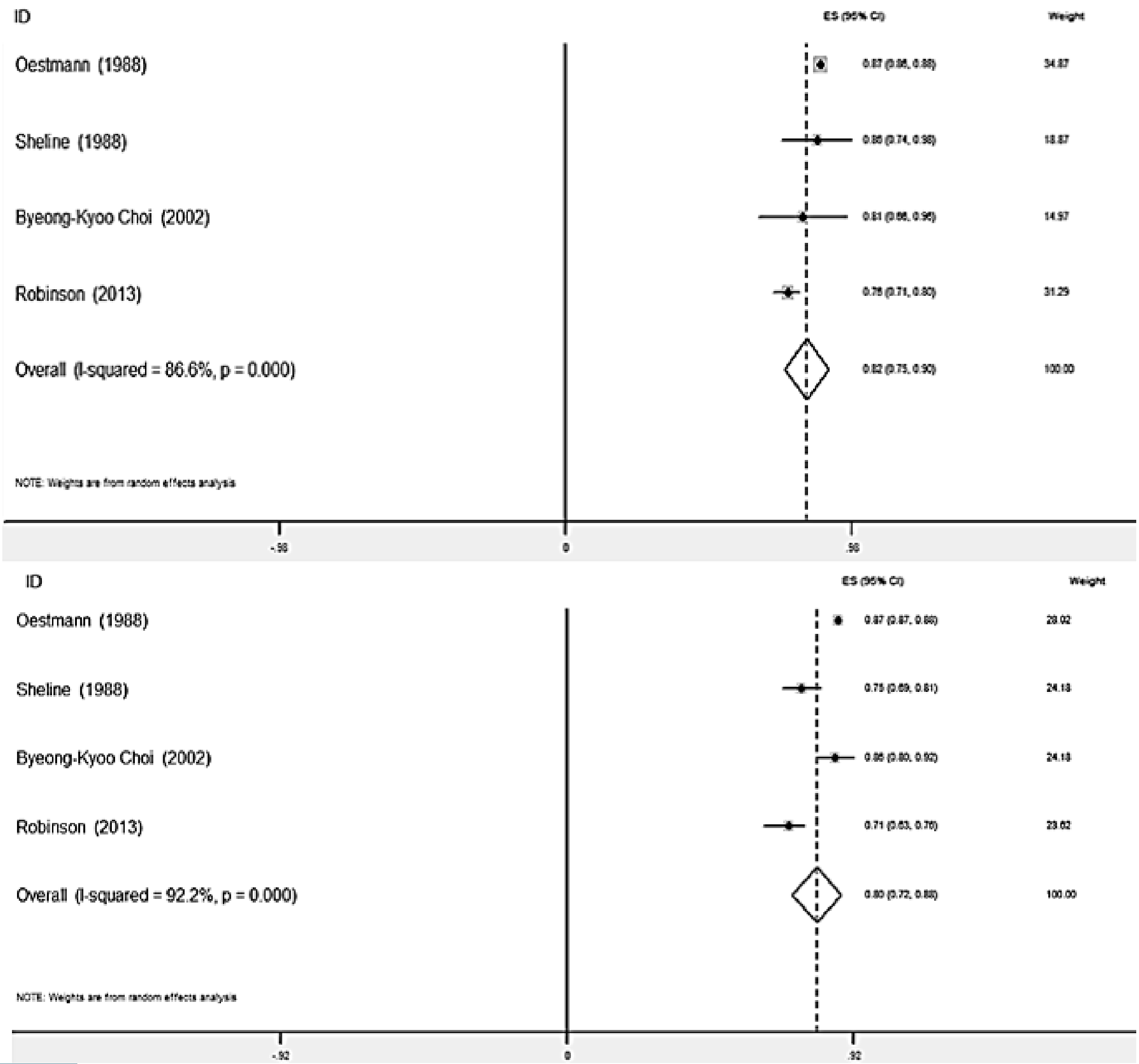

Figure 4 Conventional (below) and inverse mode (above) AUC forest plot

5. Limitations

We acknowledge several limitations in this review. Firstly, this review excluded non–English–language articles, which led to the omission of some studies. Secondly, included studies varied in target lesions, index tests, gold standards, and also the parameters reported for accuracy. Finally, due to number of studies, it was not possible to perform other analysis such as publication bias.

6. Conclusion

In summary, application of inverse mode when using radiography for detection of pulmonary nodules may improve diagnostic accuracy. Although inverse/combined mode showed better performance for other lesions in some studies, there was insufficient evidence to draw a consistent conclusion.

7. Declarations

7.1. Acknowledgement

The authors would like to thank Zhuo Qian Cao for his editorial comments on this study.

7.2. Authors' contribution

All the authors passed four criteria for authorship contribution based on recommendations of the International Committee of Medical Journal Editors.

7.3. Conflict of interest

None declared.

7.4. Funding

None declared.

Copyright © 2023 Tehran University of Medical Sciences
This work is licensed under a Creative Commons Attribution-NonCommercial 4.0 International license (https://creativecommons.org /licenses/by-nc/4.0/).
Noncommercial uses of the work are permitted, provided the original work is properly cited.

References

1. Bruno MA, Walker EA, Abujudeh HH. Understanding and confronting our mistakes: the epidemiology of error in radiology and strategies for error reduction. Radiographics. 2015;35(6):1668–76.
2. Blackwell HR. Contrast thresholds of the human eye. Josa. 1946;36(11):624–43.
3. Thompson JD, Thomas NB, Manning DJ, Hogg P. The impact of greyscale inversion for nodule detection in an anthropomorphic chest phantom: a free–response observer study. Br J Radiol. 2016;89(1064):20160249.
4. De Boo DW, Uffmann M, Bipat S, Boorsma EF, Scheerder MJ, Weber M, et al. Gray–scale reversal for the detection of pulmonary nodules on a PACS workstation. AJR Am J Roentgenol. 2011;197(5):1096–100.
5. Park JB, Cho YS, Choi HJ. Diagnostic accuracy of the inverted grayscale rib series for detection of rib fracture in minor chest trauma. Am J Emerg Med. 2015;33(4):548–52.
6. Whiting PF, Rutjes AW, Westwood ME, Mallett S, Deeks JJ, Reitsma JB, et al. QUADAS–2: a revised tool for the quality assessment of diagnostic accuracy studies. Ann Intern Med. 2011;155(8):529–36.
7. Kim KW, Lee J, Choi SH, Huh J, Park SH. Systematic review and meta–analysis of studies evaluating diagnostic test accuracy: a practical review for clinical researchers–part I. General guidance and tips. Korean J Radiol. 2015;16(6):1175–87.
8. Ryan R, Hill S. How to GRADE the quality of the evidence. Cochrane consumers and communication group. 2016;3.
9. Oestmann JW, Greene R. Digitale Radiographie in der Thoraxdiagnostik [Digital radiography in thoracic diagnosis](in German). Rofo. 1989;150(4):465–71.
10. Dolken W, Krahe T, Landwehr P, Horwitz AE, Lackner K. [A ROC analysis for comparing contrast perception in grey scale reversal of digital images]. Aktuelle Radiologie. 1991;1(1):23–7.
11. Barbat J, Messer HH. Detectability of artificial periapical lesions using direct digital and conventional radiography. J Endod. 1998;24(12):837–42.
12. Borrie F, Thomson D, McIntyre GT. Precision of measurements on conventional negative 'bones white' and inverted greyscale 'bones black' digital lateral cephalograms. Eur J Orthod. 2012;34(1):57–61.
13. Castro VM, Katz JO, Hardman PK, Glaros AG, Spencer P. In vitro comparison of conventional film and direct digital imaging in the detection of approximal caries. Dentomaxillofac Radiol. 2007;36(3):138–42.
14. Dove SB, McDavid WD. A comparison of conventional intra–oral radiography and computer imaging techniques for the detection of proximal surface dental caries. Dentomaxillofac Radiol. 1992;21(3):127–34.
15. Haak R, Wicht MJ. Grey–scale reversed radiographic display in the detection of approximal caries. J Dent. 2005;33(1):65–71.
16. Oliveira ML, Vieira ML, Cruz AD, Boscolo FN, SM DEA. Gray scale inversion in digital image for measurement of tooth length. Braz Dent J. 2012;23(6):703–6.
17. Priaminiarti M, Utomo B, Susworo R, Iskandar HB. Converting conventional radiographic examination data of trabecular bone pattern values into density measurement values using intraoral digital images. Oral Radiol. 2009;25(2):129–34.
18. Ammar KA, Shaikh A, Anigbogu M, Port SC. Breast cancer diagnosed by stress SPECT sestamibi: the role of inverse gray–scale imaging. J Nucl Cardiol. 2017;24(5):1816–8.
19. Hsu SJ, Tsai CY, Chang CJ, Hsu SW, Shibazaki M, Inada T, et al.. The analysis of grayscale inversion of in–plane driving liquid crystal mode. 14th International Display Workshops, Japan.2007;3:1711–4.
20. Richardson RL. A gray scale inverter for use with CT scanners and other imaging systems. Phys. Med. Biol. 1979;24(5):1030–2.
21. Tuncer T, Dogan S, Ozyurt F. An automated residual exemplar local binary pattern and iterative relief based COVID–19 detection method using lung X–ray image. Chemometr Intell Lab Syst . 2020;203:104054 .
22. Wachsberg RH. Inversion of the grayscale display to facilitate viewing of computed tomographic scans by sonographers. Ultrasound Q. 2008;24(3):179–80.
23. Hong J–Y, Hwang J–H, Suh S–W, Yang J–H, Kim J–R, Bae Y–G. Reliability of coronal curvature measures in premature scoliosis: comparison of 4 methods using inverted digital luminescence radiography. Spine. 2015;40(12):E701–E12.
24. Sun W, Zhou J, Qin X, Xu L, Yuan X, Li Y, et al. Grayscale inversion radiographic view provided improved intra– and inter–observer reliabilities in measuring spinopelvic parameters in asymptomatic adult population. BMC Musculoskelet Disord. 2016;17(1):411.
25. Xia C, Xu L, Xue B, Sheng F, Qiu Y, Zhu Z. Grayscale inversion view can improve the reliability for measuring proximal junctional kyphosis in adolescent idiopathic scoliosis. World Neurosurg. 2018;119:e631–e7.
26. Altunkeser A, Körez MK. Usefulness of grayscale inverted images in addition to standard images in digital mammography. BMC Med Imaging. 2017;17(1):1–6.
27. Joseph VM, Lynser D, Tiewsoh I, Dutta K, Phukan P, Daniala C. Tracheal diverticulum in SARS–CoV–2 patients on non–invasive ventilation a not so "spontaneous" cause of pneumomediastinum? an imaging pictorial presentation of two cases with review of literature. Acta Med Lit. 2021;28(2):302–7.
28. Choi BK, Lee IS, Seo JB, Lee JS, Song KS, Lim TH. The diagnosis of small solitary pulmonary nodule: comparison of standard and inverse digital images on a high–resolution monitor using ROC analysis. J Korean Radiol So. 2002;47(6):601–5.
29. Kang SS, Kim JK, Ryu JA, Choi N, Bae SJ, Kim B. Usefulness of reversed display of soft-copy abdominal radiographs for urinary calculi detection. Acta Radiol. 2004;45(3):351–6.

Copyright © 2023 Tehran University of Medical Sciences
This work is licensed under a Creative Commons Attribution-NonCommercial 4.0 International license (https://creativecommons.org /licenses/by-nc/4.0/). Noncommercial uses of the work are permitted, provided the original work is properly cited.

30. Lungren MP, Samei E, Barnhart H, McAdams HP, Leder RA, Christensen JD, et al. Gray–scale inversion radiographic display for the detection of pulmonary nodules on chest radiographs. Clin Imaging. 2012;36(5):515–21.
31. Kehler M, Albrechtsson U, Andresdottir A, Hochbergs P, Larusdottir H, Lundin A, et al. Efficacy of inverted digital luminescence radiography in evaluating chest neoplasms. Acta Radiol. 1991;32(6):442–8.
32. Kheddache S, Mansson LG, Angelhed JE, Denbratt L, Gottfridson B, Schlossman D. Digital chest radiography: should images be presented in negative or positive mode? Eur J Radiol. 1991;13(2):151–5.
33. Oestmann JW, Rubens JR, Bourgouin PM, Rhea JT, Llewellyn HJ, Greene R. Impact of postprocessing on the detection of simulated pulmonary nodules with digital radiography. Invest Radiol. 1989;24(6):467–71.
34. Robinson JW, Ryan JT, McEntee MF, Lewis SJ, Evanoff MG, Rainford LA, et al. Grey–scale inversion improves detection of lung nodules. Br J Radiol. 2013;86(1021):20110812.
35. Eken G, Misir A. Comparison of computed tomography, traction, and inverted grayscale radiographs for understanding pilon fracture morphology. Foot Ankle Int. 2021:10711007211049247.
36. Oestmann JW, Kushner DC, Bourgouin PM, Llewellyn HJ, Mockbee BW, Greene R. Subtle lung cancers: impact of edge enhancement and gray scale reversal on detection with digitized chest radiographs. Radiology. 1988;167(3):657–8.
37. Schaefer CM, Greene R, Llewellyn HJ, Mrose HE, Pile–Spellman EA, Rubens JR, et al. Interstitial lung disease: impact of postprocessing in digital storage phosphor imaging. Radiology. 1991;178(3):733–8.
38. Sheline ME, Brikman I, Epstein DM, Mezrich JL, Kundel HL, Arenson RL. The diagnosis of pulmonary nodules: comparison between standard and inverse digitized images and conventional chest radiographs. AJR Am J Roentgenol. 1989;152(2):261–3.
39. Kirchner J, Gadek D, Goltz JP, Doroch–Gadek A, Stuckradt S, Liermann D, et al. Standard versus inverted digital luminescence radiography in detecting pulmonary nodules: a ROC analysis. Eur J Radiol. 2013;82(10):1799–803.
40. Ledda RE, Silva M, McMichael N, Sartorio C, Branchi C, Milanese G, et al. The diagnostic value of grey–scale inversion technique in chest radiography. Radiol Med. 2022;18:18.
41. MacMahon H, Metz CE, Doi K, Kim T, Giger ML, Chan HP. Digital chest radiography: effect on diagnostic accuracy of hard copy, conventional video, and reversed gray scale video display formats. Radiology. 1988;168(3):669–73.
42. Musalar E, Ekinci S, Unek O, Ars E, Eren HT, Gurses B, et al. Which is better and useful modality of X–ray for diagnosis of pneumothorax at emergency setting: conventional or invert–grayscale? Am J Emerg Med. 2017;10.
43. Patel A, Haleem S, Rajakulasingam R, James SL, Davies AM, Botchu R. Comparison between conventional CT and grayscale inversion CT images in the assessment of the post–operative spinal orthopaedic implants. J Clin Orthop Trauma . 2021;21:101567.
44. Buckley KM, Schaefer CM, Greene R, Agatston S, Fay J, Llewellyn HJ, et al. Detection of bullous lung disease: conventional radiography vs digital storage phosphor radiography. AJR Am J Roentgenol. 1991;156(3):467–70.
45. Deeks JJ, Altman DG. Diagnostic tests 4: likelihood ratios. Bmj. 2004;329(7458):168–9.
46. Hosmer DW, Lemeshow S. Applied logistic regression. John Wiley & Sons. New York. 2000.
47. Boyd CA, Jayaraman MV, Baird GL, Einhorn WS, Stib MT, Atalay MK, et al. Detection of emergent large vessel occlusion stroke with CT angiography is high across all levels of radiology training and grayscale viewing methods. Eur Radiol. 2020;30(8):4447–53.

Copyright © 2023 Tehran University of Medical Sciences
This work is licensed under a Creative Commons Attribution-NonCommercial 4.0 International license (https://creativecommons.org /licenses/by-nc/4.0/). Noncommercial uses of the work are permitted, provided the original work is properly cited.

Appendix 1 Queries for records retrieval from Medline (via PubMed), Embase, Scopus and Web of Science

1. Ovid MEDLINE(R) and Epub Ahead of Print, In–Process & Other Non–Indexed Citations, Daily and Versions(R) 1946 to February 08, 2022		
Search Date: 9 February 2022		
1	((grey–scale or greyscale or grayscale or gray–scale) adj4 (inver$ or revers$ or conver$)).mp.	244
2. Embase 1974 to 2022 Week 05 (OvidSP)		
Search Date: 9 February 2022		
1	((grey–scale or greyscale or grayscale or gray–scale) adj4 (inver$ or revers$ or conver$)).mp.	348
3. EBM Reviews – Cochrane Central Register of Controlled Trials (CENTRAL) (OvidSP)		
Search Date: 9 February 2022		
1	((grey–scale or greyscale or grayscale or gray–scale) adj4 (inver$ or revers$ or conver$)).mp.	11
4. Scopus		
Search Date: 9 February 2022		
1	TITLE–ABS–KEY ((grey–scale OR greyscale OR grayscale OR gray–scale) W/4 (inver* OR revers* OR conver*)) AND (LIMIT–TO (SUBJAREA , "MEDI") OR LIMIT–TO (SUBJAREA , "NEUR") OR LIMIT–TO (SUBJAREA , "HEAL") OR LIMIT–TO (SUBJAREA , "DENT") OR LIMIT–TO (SUBJAREA , "PHAR") OR LIMIT–TO (SUBJAREA , "IMMU") OR LIMIT–TO (SUBJAREA , "NURS"))	271
5. Web of Science core collection		
Search Date: 9 February 2022		
1	TS= ((grey–scale OR greyscale OR grayscale OR gray–scale) NEAR/4 (inver* OR revers* OR conver*)) AND TS=(Sensitivity OR specificity OR Diagnos* OR "accuracy of detection")	98
	Indexes=SCI–EXPANDED, SSCI, A&HCI, ESCI Timespan=All years	
1	Medline	244
2	EMBASE	348
3	CENTRAL	11
4	Scopus	271
5	WOS	98
Total		972
Feb, 2022		
1. Ovid MEDLINE(R) and Epub Ahead of Print, In–Process, In–Data–Review & Other Non–Indexed Citations, Daily and Versions(R) 1946 to February 18, 2022		
Search Date: 20 February 2022		
1	((grey–scale or greyscale or grayscale or gray–scale) adj4 (inver$ or revers$ or conver$)).mp.	263
2	limit 1 to dt="20210207 –20220220"	22
2. Embase (embase.com)		
Search Date: 20 February 2022		
1	('grey scale' OR greyscale OR grayscale OR 'gray scale') NEAR/4 (inver* OR revers* OR conver*)	377
2	#1 AND (2022:py OR 2022:py)	28
3. EBM Reviews – Cochrane Central Register of Controlled Trials (CENTRAL) (OvidSP)		
Search Date: 20 February 2022		
1	((grey–scale or greyscale or grayscale or gray–scale) adj4 (inver$ or revers$ or conver$)).mp.	12
2	limit 1 to yr="2022–2022"	1
4. Scopus		
Search Date: 20 February 2022		
	TITLE–ABS–KEY ((grey–scale OR greyscale OR grayscale OR gray–scale) W/4 (inver* OR revers* OR conver*)) AND (LIMIT–TO (SUBJAREA , "MEDI") OR LIMIT–TO (SUBJAREA , "NEUR") OR LIMIT–TO (SUBJAREA , "HEAL") OR LIMIT–TO (SUBJAREA , "DENT") OR LIMIT–TO (SUBJAREA , "PHAR") OR LIMIT–TO (SUBJAREA , "IMMU") OR LIMIT–TO (SUBJAREA , "NURS")) AND (LIMIT–TO (PUBYEAR , 2022) OR LIMIT–TO (PUBYEAR , 2021))	
28		
5. Web of Science core collection		
Search Date: 20 February 2022		
	TS= ((grey–scale OR greyscale OR grayscale OR gray–scale) NEAR/4 (inver* OR revers* OR conver*)) AND TS=(Sensitivity OR specificity OR Diagnos* OR "accuracy of detection")	
Indexes=SCI–EXPANDED, SSCI, A&HCI, ESCI Timespan=2021–2022		
17		
1	Medline	22
2	EMBASE	28
3	CENTRAL	1
4	Scopus	28
5	WOS	17
Total		96
40 duplicates were removed and 56 records remained.		

Copyright © 2023 Tehran University of Medical Sciences
This work is licensed under a Creative Commons Attribution-NonCommercial 4.0 International license (https://creativecommons.org /licenses/by-nc/4.0/). Noncommercial uses of the work are permitted, provided the original work is properly cited.